INTERNATIONAL JOURNAL OF ADAPTIVE CONTROL AND SIGNAL PROCESSING
Int. J. Adapt. Control Signal Process. (2015)
Published online in Wiley Online Library (wileyonlinelibrary.com). DOI: 10.1002/acs.2566

Fault-tolerant control of an air heating fan using set-valued observers: An experimental evaluation

Paulo Rosa[1,*,†], Tiago Simão[4,5], Carlos Silvestre[2,3] and João M. Lemos[4,5]

[1]*Deimos Engenharia, 1998-023 Lisboa, Portugal*
[2]*Department of Electrical and Computer Engineering, Faculty of Science and Technology, University of Macau, Taipa, Macau, China*
[3]*Institute for Systems and Robotics-Instituto Superior Técnico, Lisbon 1049-001, Portugal*
[4]*INESC-ID, 1049-001 Lisboa, Portugal*
[5]*Instituto Superior Tecnico, 1049-001 Lisboa, Portugal*

SUMMARY

This paper proposes a multiple-model solution to the problem of controlling an air heating fan subject to faults. These faults are modeled by means of an abnormal unknown airflow input rate which the nominal controller is not designed for. Moreover, the average temperature of the air flowing through the system, which can be seen as an offset on the corresponding dynamics, is (slowly) time-varying and highly dependent on the ambient temperature. The fault-tolerant control (FTC) method adopted makes use of set-valued observers (SVOs) to invalidate possible models of the system. Unlike classical fault detection, this approach does not rely on residuals to detect abnormal system operation. This fact allows to reduce the conservatism of the solution and enables a straightforward design from the faulty and nominal models of the plant. Moreover, the absolute distinguishability concept is used to derive input signals that bolster the detection of faults. Although SVOs require heavy real-time calculations that hinder its implementability in systems with low computational power, it is shown that the architecture of the FTC strategy proposed is highly parallelizable and, thus, may take advantage of standard multi-core processing units. Experimental results are presented.

Received 5 August 2013; Revised 10 March 2015; Accepted 11 April 2015

KEY WORDS: fault tolerant control; multiple-model; set-valued observers; fault distinguishability

1. INTRODUCTION

Fault-tolerant control (FTC) systems play an increasingly more important role in the field of control, particularly because of the also increasing complexity of the systems to be controlled. In addition to adequate disturbance-rejection under nominal operation, safety critical systems – such as flight control systems or nuclear power plants – require fast fault detection and accommodation so that human and material damage is minimized.

This objective can typically be achieved either by using *active* or *passive* FTC methodologies, or even by adopting hybrid solutions. Passive fault-tolerant control (PFTC) methods assume, during the design of the controllers, that the system can either be healthy or faulty and that the controller must be able to handle both scenarios, thus leading to a reduced nominal performance. Notwithstanding the robustness guarantees yielded by these controllers, faults with large magnitudes are unlikely to be properly handled, without significantly degrading the closed-loop performance of the system. Thus, this paper focuses on a so-called active fault-tolerant control (AFTC) methodology.

*Correspondence to: Paulo Rosa, Deimos Engenharia, Av. D. João II, Lt 1.17.01, Andar 10, 1998-023 Lisboa, Portugal.
†E-mail: prosa@isr.ist.utl.pt

Active fault-tolerant control architectures are characterized by being able to reconfigure (see [1–3] and references therein) the controller in the presence of faults. This can be performed by the controller itself or by relying on a fault detection and isolation (FDI) system to detect and evaluate the magnitude of a fault. In the latter case, the performance of the AFTC system is, therefore, highly dependent upon the performance of the associated FDI scheme. As a consequence, mixed active–passive FTC solutions have appeared in the literature – see, for instance, [4, 5] – that use a PFTC system until a fault is detected, while switching to a low-performance high-robustness controller when a fault is detected and until it is isolated and identified. From that moment onwards, a high-performance reconfigurable controller is used. A similar solution can also be found in the literature of adaptive control – the so-called safe switching adaptive control [6] – where a controller can only be connected to the plant if it is guaranteed to render the closed-loop stable.

A myriad of alternative solutions to FDI and FTC have been proposed by the scientific community in the last three decades. The reader is referred to [1–3] and [7] for a thorough comparison of the methods available in the literature.

This paper addresses the problem of designing an FTC for an air heating fan that can be used to model, for instance, air-conditioning systems. The plant considered is a Process Trainer PT326 developed by Feedback Instruments Limited (5 & 6 Warren Court, Crowborough, East Sussex, TN6 2QX, UK) [8] (Figure 1). The atmospheric air is drawn by a blower (on the left) and passes through a heater (①) and a tube (②) before returning to the atmosphere. The goal is to regulate the temperature of the air, $T(\cdot)$ – sensed by a thermistor with output variable $y(\cdot)$, measured in volt – using the heater (①) in Figure 1, with manipulated input voltage signal $u(\cdot)$.

The air flow $q(\cdot)$ can be manually manipulated by changing the throttle opening (θ°) from 10° to 165° (degrees), and as shown in the sequel, has a significant impact on the dynamic behavior of the system. Minimum and maximum throttle openings, $\theta_{\min} = 10^\circ$ and $\theta_{\max} = 165^\circ$, correspond to minimum and maximum flows, respectively. Finally, the system is also affected by the ambient temperature T_a. However, this (uncontrollable) variable is only responsible for generating a (slowly) time-varying offset on the output, and hence, it does not change the incremental dynamics of the plant. Still, this drifting operating point hinders the detectability of faults, as a highly sensitive FDI system may lead to an arbitrary number of false alarms because of these offset variations.

The nonlinear model of the system is approximated by scheduling between several local models, each of which corresponds to a pre-specified set of values of the throttle opening. Figure 2 depicts the responses of the system, for three different throttle openings (30°, 70°, and 130°), to a square-wave input signal, using a sampling frequency of 1 kHz. The different offsets of the measured variable, $y(\cdot)$, are related to each operating point, and are (slowly) time-varying and highly dependent on the ambient temperature, T_a. Therefore, these offsets cannot be used for the identification of the plant dynamics.

The solution adopted in this paper falls within the realm of active FTC, because a passive controller able to accommodate all the types of faults considered would yield a significantly degraded performance. In particular, we take advantage of the recent advances in the set-valued observers (SVOs) theory to invalidate models of the plant that are not compatible with the current input/output sequences, as described in the sequel – see [9–11]. Once a fault is detected and isolated, a controller

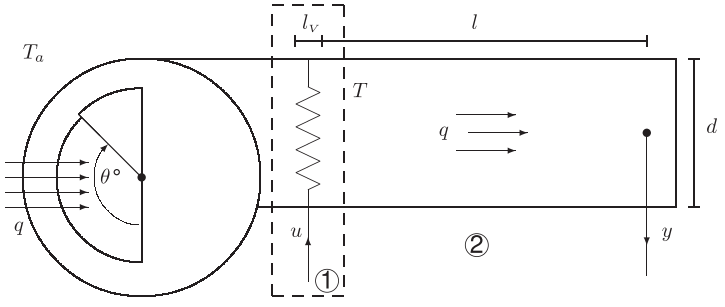

Figure 1. Scheme of an air-heating system.

DOI: 10.1002/acs

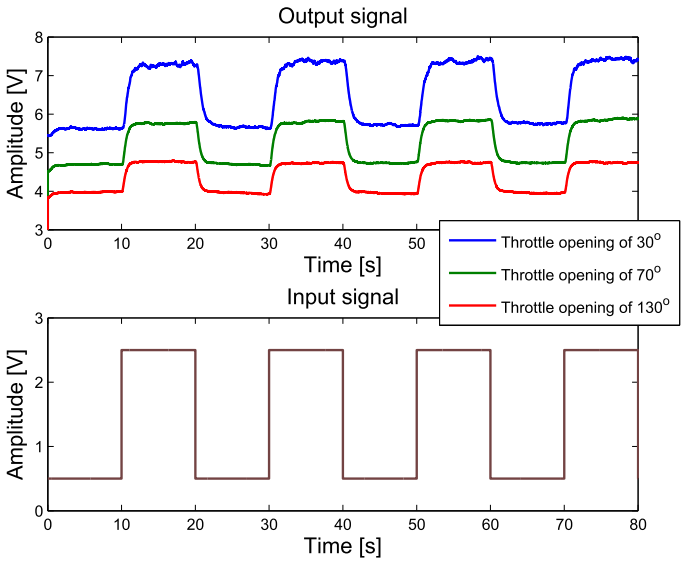

Figure 2. System response to a square-wave input signal for the three throttle openings and a sample period of 1 ms.

synthesized for the impaired system is connected to the loop. This paper builds on the results presented in [12], by providing a thorough description of the methodology adopted.

1.1. Main contributions

The main contributions of this paper are as follows:

- The development of a multiple-model dynamic description for the Process Trainer PT326.
- The application of a novel AFTC design methodology for linear parameter-varying (LPV) systems, with guaranteed closed-loop stability, and that also allows faulty-to-healthy transitions of the process.
- The adoption of the concept of absolute distinguishability to discern between signals that enable the detection of faults.
- The experimental evaluation of the proposed solution in a distributed computational setup, illustrating the applicability of the FTC solution adopted to real-time systems.
- The demonstration of an approach to FTC based on multiple-models and SVO that is able to run in real-time.

In addition to closed-loop stability, the proposed technique also provides improved performance when compared with a passive FTC approach. Moreover, it is shown that the deterioration, in terms of performance, when compared with the (non-realizable) perfect model identification scheme, is negligible, at least in the scenarios considered in this paper.

1.2. Organization of the paper

This paper is organized as follows. Section 2 describes the dynamics of the air heating fan and presents the derivation of a multiple-model uncertain description of the system. The SVO-based approach to FTC is introduced in Section 3, and the experimental results are presented in 4. Finally, some conclusions regarding the proposed technique are discussed in Section 5.

2. DYNAMICS OF THE AIR HEATING FAN

For each operating scenario, the dynamics of the Process Trainer PT326, illustrated in Figure 1, was discretized with a zero-order hold and a sampling period of 200 ms, and modeled by the autoregressive-moving-average model (ARMAX) structure described by

DOI: 10.1002/acs

$$y(k) + a_1\, y(k-1) + \ldots + a_{n_a}\, y(k-n_a) = b_1\, u(k-n_k) + \ldots + b_{n_b}\, u(k-n_k-n_b+1) + e(k) + c_1\, e(k-1) + \ldots + c_{n_c}\, e(k-n_c), \tag{1}$$

where $y(\cdot)$ is the measured temperature, $u(\cdot)$ is the control input, that is, the power delivered to the heater, and $e(\cdot)$ is a white Gaussian process noise. The coefficients a_i, b_j, and c_m were experimentally assessed.

For all the (local) models considered, we used $n_a = n_c = 3$ and $n_b = 2$. Finally, the delay n_k is different for each of those models. These $ARMAX$ models can be described in state-space form by

$$\tilde{S}_i : \begin{cases} \tilde{x}_i(k+1) &= \tilde{A}_i \tilde{x}_i(k) + \tilde{B}_i u(k) \\ \tilde{y}_i(k) &= \tilde{C}_i \tilde{x}_i(k) + n_i(k) + b_i(k) \end{cases}, \tag{2}$$

where i denotes the index of the local model, $b_i(k) \in \mathbb{R}$ is the offset of the output variable, $n_i(k)$ is the measurement noise, and $\tilde{x}_i$ is the state of the associated local model, at time k. For each value of the throttle opening, a different set of state-space matrices is obtained.

Figure 3(a) depicts the outputs of three different models (30°, 70°, and 130°) obtained in simulation, for the throttle opening sequence 130° → 70° → 130° → 30° → 70° → 30° → 130°, that changes every 50 s. The simulation results are obtained by considering a dynamic model given by

$$\tilde{S} : \begin{cases} \tilde{x}(k+1) &= \tilde{A}_{\sigma(k)} \tilde{x}(k) + \tilde{B}_{\sigma(k)} u(k) \\ \tilde{y}(k) &= \tilde{C}_{\sigma(k)} \tilde{x}(k) + n(k) + b_{\sigma(k)}(k) \end{cases}, \tag{3}$$

where $\sigma(k)$ denotes the operating point and, thus, is directly related to the throttle opening. The measured output of the plant, obtained with the experimental setup, and using the same throttle opening sequence, is illustrated in Figure 3(b). The state-space matrices of the aforementioned models are given by

$$\tilde{A}_1 = \begin{bmatrix} 1.4599 & -0.7869 & 0.1853 \\ 1 & 0 & 0 \\ 0 & 1 & 0 \end{bmatrix}, \quad \tilde{B}_1 = \begin{bmatrix} 1 \\ 0 \\ 0 \end{bmatrix}, \quad \tilde{C}_1 = \begin{bmatrix} 0.0101 & 0.1070 & 0 \end{bmatrix},$$

$$\tilde{A}_2 = \begin{bmatrix} 0.8571 & -0.1832 & 0.0309 \\ 1 & 0 & 0 \\ 0 & 1 & 0 \end{bmatrix}, \quad \tilde{B}_2 = \begin{bmatrix} 1 \\ 0 \\ 0 \end{bmatrix}, \quad \tilde{C}_2 = \begin{bmatrix} 0.0638 & 0.0962 & 0 \end{bmatrix},$$

$$\tilde{A}_3 = \begin{bmatrix} 0.6332 & 0.0428 & -0.0381 \\ 1 & 0 & 0 \\ 0 & 1 & 0 \end{bmatrix}, \quad \tilde{B}_3 = \begin{bmatrix} 1 \\ 0 \\ 0 \end{bmatrix}, \quad \tilde{C}_3 = \begin{bmatrix} 0.0754 & 0.0673 & 0 \end{bmatrix}.$$

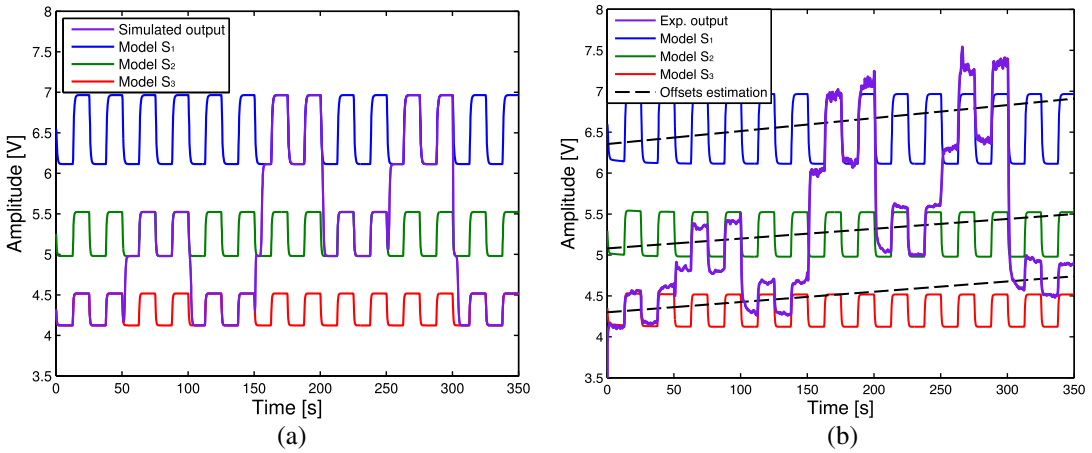

Figure 3. Simulated (a) and experimental (b) output of the plant. $\tilde{S}_1$, $\tilde{S}_2$, and $\tilde{S}_3$ were obtained for throttle openings of 30°, 70°, and 130°, respectively.

DOI: 10.1002/acs

We consider that the nominal operation of the system is yielded at a throttle opening of $\theta \in [60°,\ 120°[$. All of the other scenarios are considered abnormal situations and thus can be interpreted as faults. It is important to stress, however, that these types of faults have a direct impact not only on the actuation but also on the dynamics of the system $(\tilde{A}_i, \tilde{C}_i)$.

Remark 1
It should be noticed that the overheating of the tube has an impact on the offsets of all models over time. Indeed, this overheating effect causes a variable offset in each model that is apparent from Figure 3(b).

3. SET-VALUED OBSERVER-BASED FAULT-TOLERANT CONTROL

The large level of uncertainty of the model of the air heating fan significantly hinders the problem of designing a single *non-adaptive* controller for all the admissible models of the plant. To overcome this issue, several solutions are proposed in the literature of adaptive control based on a single plant model (cf. [13–17]), and in the literature of FTC systems (cf. [1–3]).

In this paper, however, the focus is on a class of adaptive control architectures, referred to as multiple-model adaptive control (MMAC). In terms of design, the idea behind the MMAC is to split the (large) set of parametric uncertainty, Ω, into N_S (small) subregions, Ω_i, $i \in \{1, \cdots, N_S\}$ – see Figure 4 for an example where a single uncertain parameter is considered – and a non-adaptive controller for each of these subregions is synthesized. In terms of implementation, the goal is set to identify which region the uncertain parameters, ρ, belong to and then connect to the loop the controller designed for that region – see [18–20], and references therein.

Thus, multiple-model control techniques aim to select, at each time instant, a controller that is capable of yielding the desired stability and performance levels. Moreover, the transition between controllers must be executed in such a way that no instability issues arise.

Multiple-model architectures enjoy several advantages [21], such as the fast adaptation, compared with indirect adaptive control (see [22–24], and references therein), when the plant dynamics change abruptly (for instance, because of failures), and the ability to provide high levels of performance for different classes of dynamic models. Furthermore, multiple-model approaches have a design modularity that makes them suitable for a number of applications, while being able to provide a natural accommodation of faults. In particular, multiple-model architectures provide a natural way of embedding the control objective configuration that can be crucial when accommodating faults [25]. Because of their solid theoretical background, these methodologies are also able to provide closed-loop stability and performance robustness guarantees under time-variations of the parameters, thus rendering this methodology appropriate for safety critical applications, such as FTC of flight systems.

Several MMAC architectures have been proposed that provide stability and/or performance guarantees, as long as a set of assumptions are met. For instance, [19] uses a parameter estimator to select a controller, guaranteeing stability of the closed-loop. Another MMAC approach, referred to as robust multiple-model adaptive control (RMMAC), that was introduced in [26] and references therein, uses a bank of Kalman filters for the identification system and a hypothesis testing strategy to select the controllers. For this case, although simulation results – see, for instance, [26] – indicate that high levels of performance are obtained, the only guarantees that can be provided are in terms of stability – see [27, 28]. In [29], calibrated forecasts are used to guarantee the stability of the closed-loop. This approach was later on extended in [30], to provide stability guarantees for several

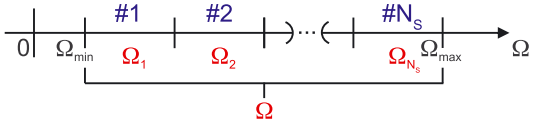

Figure 4. Uncertainty region, Ω, for the parameter ρ, split into N_S subsets, $\Omega_i, i = \{1, \cdots, N_S\}$.

DOI: 10.1002/acs

MMAC architectures. The theory of unfalsified control – see [31–35], among others [36, 37] – uses the controlled output error to decide whether the selected controller is delivering the desired performance or not. Other MMAC approaches increase the number of uncertainty regions in order to improve performance, whenever a given condition is satisfied (cf. [38]).

The approach adopted in this article uses a line-of-thought similar to that of the unfalsified control theory. Rather than trying to identify the *correct* region of uncertainty, by hypothesis testing or parameter estimation, the *wrong* regions are excluded. In other words, if the time-evolution of the inputs and outputs of the plant cannot be explained by a model with uncertain parameter ρ, such that $\rho \in \Omega_i$, then region Ω_i cannot be the one to which the uncertain parameter belongs. The invalidation of these uncertainty regions is addressed by using SVOs, taking advantage of the recent developments presented in [9, 10, 39, 40].

In summary, the approach provided in this paper is to use SVOs to detect faults by looking for inconsistencies between the input/output sequences – similarly to what is performed in [11] – and to decide which non-adaptive controllers should *not* be selected. The selection among the *non-invalidated* controllers may be performed by using an auxiliary decision algorithm, or by using a pre-routed approach – see [30]. Similarly to other MMAC architectures, we use a bank of observers – in our case, SVOs – each of which *tuned* for a pre-specified region of uncertainty.

It should be noticed that the number of uncertainty regions is key in terms of the time required to select the appropriate controller to be connected to the loop, as derived in [30] for a class of time-varying nonlinear systems. This limitation has been recognized in the controls community (see, for instance, [21]) and several methods have, since then, been developed to reduce this search to a small number of regions of uncertainty. In this paper, this issue is approached by using the notion of *absolute input-distinguishability*, described in the sequel, which can be seen as a tool to properly *split* the parameter space into the a number of sub-regions, ensuring the invalidation of all but the 'correct' model of the plant within a pre-specified time-horizon.

3.1. Preliminaries and notation

The class of systems considered in this paper, typically referred to as uncertain LPV systems, can be described by

$$\begin{cases} x(k+1) = A(k,\rho(k))x(k) + B(k,\rho(k))u(k) + L(k,\rho(k))d(k) \\ \quad y(k) = C(k,\rho(k))x(k) + N(k,\rho(k))n(k), \end{cases} \tag{4}$$

where $x(0) \in X(0)$, $x(k) \in \mathbb{R}^n$, $d(k) \in \mathbb{R}^{n_d}$, $n(k) \in \mathbb{R}^{n_n}$, $u(k) \in \mathbb{R}^{n_u}$, and $y(k) \in \mathbb{R}^{n_y}$, for $k \geqslant 0$. The (partially) uncertain time-varying vector of parameters, $\rho(\cdot)$, is such that $\rho(k) \in \mathbb{R}^{n_\rho}$. It is also assumed that $|d(k)| := \max_i |d_i(k)| \leqslant 1$, and $|n(k)| := \max_i |n_i(k)| \leqslant \bar{n}$. At each time, k, the vector of states is denoted by $x(k)$, and we define $X(0) := \mathrm{Set}(M_0, m_0)$, where

$$\mathrm{Set}(M,m) := \{q : Mq \leqslant m\} \tag{5}$$

represents a convex polytope. As an additional constraint, it is assumed that the matrices of the dynamics depend affinely on the vector of parameters.

Let $\mathcal{S}$ denote the set of *plausible* or *admissible* models of the plant to be controlled. We assume that $\mathcal{S}$ is a finite set, with cardinality N_S, and that each $S_i \in \mathcal{S}$ can be described by

$$S_i : \begin{cases} x_i(k+1) = A_i(\rho(k))x_i(k) + B_i(\rho(k))u(k) + L_i(\rho(k))d_i(k), \\ \quad y_i(k) = C_i(\rho(k))x_i(k) + N_i(\rho(k))n_i(k), \end{cases} \tag{6}$$

for each $i \in \{1, \cdots, N_S\}$, with $\rho(k) \in \Omega_i$ for all $k \geqslant 0$, and using a nomenclature similar to that of (4). Moreover, for any $i, j \in \{1, \cdots, N_S\}$, it is clear that

$$S_i = S_j \Leftrightarrow \Omega_i = \Omega_j.$$

DOI: 10.1002/acs

Define W_d, W_n, and U, such that $d_i(j) \in W_d \subseteq \mathbb{R}^{n_d}$, $n_i(j) \in W_n \subseteq \mathbb{R}^{n_n}$, and $u(j) \in U \subseteq \mathbb{R}^{n_u}$, for all times j. The initial state of system S_i is represented by $x_o^i := x_i(0) \in X(0) := X_o \subseteq \mathbb{R}^n$. The sets W_d, W_n, and U are assumed to be compact convex polytopes, and we define $W := W_d \times W_n$.

3.2. Design of set-valued observers

Let $X(k+1)$ represent the set of possible states at time $k+1$, that is, the state $x(k+1)$ satisfies (4) with $x(k) \in X(k)$ if and only if $x(k+1) \in X(k+1)$. The goal of an SVO is to find $X(k+1)$ based upon (4) and with the additional knowledge that $x(k) \in X(k), x(k-1) \in X(k-1), \cdots, x(k-N) \in X(k-N)$, for some finite horizon N. We further require that, for all $x \in X(k+1)$, there exists $x^\star \in X(k)$ such that, for $x(k) = x^\star$, the observations are compatible with (4). In other words, we want $X(k+1)$ to be the smallest set containing all the solutions to (4).

The problem of designing this type of observer has been extensively analyzed in the literature. One of the first algorithms developed to compute (ellipsoidal) set-valued estimates of the state of a system was introduced in [41] and [42]. In [43], an approach to the synthesis problem of SVOs for linear time-varying plants with nonlinear equality constraints is described. A method for active mode observation of switching systems, based on SVOs, has been recently proposed in [44]. Another solution, applicable to LPV systems, is presented in [45]. Alternative methods have also been proposed in [46–49] and references therein. Recent improvements in observer design techniques based on interval analysis have also led to interesting results in terms of applicability to continuous and discrete, time-varying linear systems, either with continuous or discrete-time measurements, as shown in [50, 51] and references therein.

The solution adopted in this paper is an alternative to the aforementioned approaches, which provides set-valued state estimates that are guaranteed to contain the *true* state of the system. It is based on the procedure introduced in [52], for discrete time-varying linear systems, and extended to uncertain plants in [9] and [10]. Given that it can take into account values of the horizon, N, greater than 1, it typically leads to reduced conservatism, when compared with interval-analysis methods. This is obtained, however, at the cost of increased computational requirements.

For plants with uncertainties, the set $X(k+1)$ is, in general, non-convex, even if $X(k)$ is convex. Thus, it cannot be represented by a linear inequality as in (5). The approach suggested in [9] is to overbound this set by a convex polytope, $\hat{X}(k+1)$, therefore adding some conservatism to the solution. A different method was presented in [10, 11], which requires a smaller computational effort, while reducing the conservatism of the solution. Throughout the remainder of this article, we are going to use the latter approach, in order to compute set-valued state estimates, $\hat{X}(k)$, of dynamic systems that can be modeled by (4).

For the sake of completeness, a brief description of the main reasoning behind the SVO synthesis methodology is presented in the sequel. As previously mentioned, the computation of $X(k+1)$ based upon $X(k)$ for systems with no model uncertainty can be performed by using the technique described in [52]. Indeed, consider the dynamics of the plant are described by (4), and assume that the matrices of the dynamics are exactly known, although possibly time-varying. For the sake of simplicity, assume that $N(k, \rho(k)) = I$, and that $A(k, \rho(k)) := A(k)$, $B(k, \rho(k)) := B(k)$, $C(k, \rho(k)) := C(k)$ and $L(k, \rho(k)) := L(k)$. In other words, assume that, at this point, the dynamics do not depend on the uncertain vector of parameters, $\rho(k)$. Then, $x(k+1) \in X(k+1)$ if and only there exist $x(k)$ and $d(k)$, such that, for the current measurement, $y(k+1)$, we have

$$P(k) \begin{bmatrix} x(k+1) \\ x(k) \\ d(k) \end{bmatrix} \leqslant \begin{bmatrix} B(k)u(k) \\ -B(k)u(k) \\ \bar{d} \\ \bar{d} \\ \tilde{m}(k) \\ m(k-1) \end{bmatrix} =: p(k), \tag{7}$$

DOI: 10.1002/acs

where

$$P(k) := \begin{bmatrix} I & -A(k) & -L(k) \\ -I & A(k) & L(k) \\ 0 & 0 & I \\ 0 & 0 & -I \\ \tilde{M}(k) & 0 & 0 \\ 0 & M(k-1) & \end{bmatrix}, \quad \tilde{M}(k) = \begin{bmatrix} C(k) \\ -C(k) \end{bmatrix}, \quad \tilde{m}(k) = \begin{bmatrix} \bar{n} + y(k+1) \\ \bar{n} - y(k+1) \end{bmatrix},$$

and where $M(k-1)$ and $m(k-1)$ are defined such that $X(k) = \text{Set}\,(M(k-1), m(k-1))$. The inequality in (7) provides a description of a set in $\mathbb{R}^{2n+n_d}$, denoted by

$$\Gamma(k+1) = \text{Set}\,(P(k), p(k))\,.$$

Therefore, it is straightforward to conclude that

$$\hat{x} \in X(k+1) \Leftrightarrow \underset{x \in \mathbb{R}^n, d \in \mathbb{R}^{n_d}}{\exists} : \begin{bmatrix} \hat{x} \\ x \\ d \end{bmatrix} \in \Gamma(k+1).$$

Hence, the set $X(k+1)$ can be obtained by projecting $\Gamma(k+1)$ onto the subspace of the first n coordinates, which can be attained by resorting to the so-called *Fourier–Motzkin elimination method* [52, 53]. Therefore, a description of all the admissible $x(k+1)$ is obtained that does not depend upon specific $x(k)$ nor $d(k)$.

As shown in [11, 54, 55] the relationship described by (7) can be readily extended to the case where not only $X(k)$ but also $X(k-1), \cdots, X(k-N)$ are used for the estimation of $X(k+1)$. This strategy allows us to reduce the conservatism of the method when, in order to constrain the complexity of the set $X(k+1)$, an overbound $\hat{X}(k+1)$ is computed instead. The application of this technique to uncertain systems is described, for instance, in [39, 54].

3.3. Absolute input distinguishability

As previously mentioned, the proper selection of the uncertainty regions is of prime importance for the type of control strategy adopted. In particular,

- the number of models, N_S, should be kept small, in order to reduce the length of transients;
- the uncertainty regions should be sufficiently small, so that the local controllers ensure the required performance levels; and
- the exogenous signals should sufficiently excite the dynamics of the plant, in order to allow for the identification of the *best* model of the system, from the set of admissible systems.

Therefore, this section aims to derive, for a pre-specified type of input signals, the largest size of an uncertainty region, Ω_i, that enables its invalidation (or falsification), in case the *true* parameter does not belong to that set, that is, $\rho \notin \Omega_i$. The following notion of *distinguishability* will be used in this paper to provide an upper bound on the time required to detect a given fault.

Definition 1 ([56]*)*
Let $d_i^j = d_j(i)$ and $n_i^j = n_j(i)$. Systems S_1 and S_2 are said to be *absolutely* (X_o, U, W)*-input distinguishable in* N *measurements* if, for any non-zero

$$\left(x_o^1, x_o^2, d_{0,N-1}^1, d_{0,N-1}^2, n_{0,N}^1, n_{0,N}^2, u_{0,N-1},\right) \in X_o^2 \times W_d^{2N} \times W_n^{2(N+1)} \times U^N,$$

there exists $k \in \{0, 1, \cdots, N\}$ such that

$$y_1(k) \neq y_2(k).$$

DOI: 10.1002/acs

Moreover, two systems are said to be *absolutely* (X_o, U, W)*-input distinguishable* if there exists $N \geqslant 0$ such that they are absolutely (X_o, U, W)-input distinguishable in N measurements.

In the definition, we used the short-hand notation $v_{0,N}$ to denote a concatenation of a sequence of vectors

$$v_{0,N} := \left[v_o^T, \cdots, v_N^T\right]^T.$$

Unlike other definitions of distinguishability that can be found in the literature [57–59], Definition 1 is important when we want to guarantee that, regardless of the input signals, two systems can be distinguished in a given number of measurements.

The derivation of sufficient conditions for distinguishability typically leads to cumbersome calculations. In particular, in [56], a method is proposed that formulates the distinguishability problem as a concave optimization program, in order to obtain bounds on the intensity of the disturbances that guarantee the distinguishability of two dynamic systems. An alternative solution is proposed in [44], by deriving control input signals that lead to the identifiability of the system at hand.

The approach proposed in this paper is to assess which frequency ranges of the input signal are more favorable in terms of distinguishability, as described in the sequel. If the input signals indeed have the frequency content that enables the distinguishability of the possible models of the system, one can ensure that all except the 'correct' model are invalidated. The following result will be used to guarantee that, if two signals render two linear time-invariant (LTI) systems distinguishable, then so does the sum of those signals.

Proposition 1
Consider that systems S_1 and S_2, with sampling period T_s, are single-input/single-output LTI and (X_o, U, W)-input distinguishable in N measurements, where

$$X_o = \{0\}, \quad W = \{0\} \times W_n,$$

and

$$U = \{u(0), u(1), \cdots | u(k) = u_1 \sin(\omega k T_s)\} \bigcup \{u(0), u(1), \cdots | u(k) = u_2 \sin(\tilde{\omega} k T_s)\},$$

with $\omega \neq \tilde{\omega}$ and with $W_n = [-\bar{n}, \bar{n}]$. Then, for sufficiently large $\bar{N}$ and sufficiently small $T_s > 0$, systems S_1 and S_2 are $(X_o, \bar{U}, W)$-input distinguishable in $\bar{N}$ measurements, where

$$\bar{U} = U \bigcup \{u(0), u(1), \cdots | u(k) = u_1 \sin(\omega k T_s) + u_2 \sin(\tilde{\omega} k T_s)\}.$$

Proof
Define $t = kT_s$, where T_s is the sampling period, and let $y_1(\cdot)$ and $\tilde{y}_1(\cdot)$ denote the responses of S_1 to $u(k) = u_1 \sin(\omega k T_s)$ and $u(k) = u_2 \sin(\tilde{\omega} k T_s)$, respectively, with analogous definition of $y_2(\cdot)$ and $\tilde{y}_2(\cdot)$ for system S_2. Then, for some $a_1, \tilde{a}_1, a_2, \tilde{a}_2 \in \mathbb{R}^+$ and $b_1, \tilde{b}_1, b_2, \tilde{b}_2 \in [0,\ 2\pi[$,

$$\begin{cases} y_1(t) = a_1 \sin(\omega t + b_1) \\ \tilde{y}_1(t) = \tilde{a}_1 \sin(\tilde{\omega} t + \tilde{b}_1) \end{cases}$$

and

$$\begin{cases} y_2(t) = a_2 \sin(\omega t + b_2) \\ \tilde{y}_2(t) = \tilde{a}_2 \sin(\tilde{\omega} t + \tilde{b}_2) \end{cases}$$

Because the two systems are distinguishable using either input signals, it is straightforward to conclude that

$$|y_1(t_1) - y_2(t_1)| \geqslant 2\bar{n} \text{ for some } t_1 \leqslant N T_s, \tag{8}$$

and

$$|\tilde{y}_1(t_2) - \tilde{y}_2(t_2)| \geqslant 2\bar{n} \text{ for some } t_2 \leqslant N T_s. \tag{9}$$

DOI: 10.1002/acs

Now, consider the responses of each system to the input signal $u(k) = u_1 \sin(\omega k T_s) + u_2 \sin(\tilde{\omega} k T_s)$, which can be written as

$$\hat{y}_1(t) = a_1 \sin(\omega t + b_1) + \tilde{a}_1 \sin(\tilde{\omega} t + \tilde{b}_1),$$

and

$$\hat{y}_2(t) = a_2 \sin(\omega t + b_2) + \tilde{a}_2 \sin(\tilde{\omega} t + \tilde{b}_2).$$

Hence,

$$\begin{aligned} \hat{y}_1(t) - \hat{y}_2(t) &= a_1 \sin(\omega t + b_1) + \tilde{a}_1 \sin(\tilde{\omega} t + b_2) - a_2 \sin(\omega t + b_2) - \tilde{a}_2 \sin(\tilde{\omega} t + \tilde{b}_2) \\ &= A_1 \sin(\omega t + c_1) - A_2 \sin(\tilde{\omega} t + c_2), \end{aligned}$$

for some $A_1, A_2 \in \mathbb{R}^+$, and $c_1, c_2 \in [0,\ 2\pi[$.

However, $A_1 \geqslant 2\bar{n}$ and $A_2 \geqslant 2\bar{n}$ for (8) and (9) to be satisfied, respectively. Therefore,

$$|\hat{y}_1(t) - \hat{y}_2(t)| \geqslant 2\bar{n} |\sin(\omega t + c_1) - \sin(\tilde{\omega} t + c_2)|.$$

According to Lemma 1 in the Appendix, there exists $t_3 \in \mathbb{R}^+$ such that

$$|\sin(\omega t_3 + c_1) - \sin(\tilde{\omega} t_3 + c_2)| > 1.$$

Hence, it is straightforward to conclude that, by continuity of $\sin(\cdot)$, for sufficiently small T_s, there exists k_3 such that

$$|\sin(\omega k_3 T_s + c_1) - \sin(\tilde{\omega} k_3 T_s + c_2)| > 1,$$

which completes the proof. □

Remark 2
Proposition 1 assumes that no disturbances are acting upon the system. Otherwise, these exogenous signals may hinder the distinguishability problem. Measurement noise, however, is considered.

Remark 3
Although Proposition 1 only provides sufficient conditions for distinguishability, it can be trivially shown that, if one of the assumptions is violated, one may end up with signals that do not enable distinguishability. For instance, if both input signals have the same frequency, it is possible that they cancel out, which obviously prevents the system from being excited. Alternatively, if, for instance, $\tilde{\omega} = 2\omega$ and $T_s \geqslant \pi/\omega$, then the responses of the two systems may be identical at sampling times.

Remark 4
As a final remark, it is stressed that $\bar{N}$ may be larger than N. As an example, consider that $|\omega - \tilde{\omega}|$ is small, and that $b_1 - \tilde{b}_1 = b_2 - \tilde{b}_2 = \pi$ and $a_1 = \tilde{a}_1 = a_2 = \tilde{a}_2$. Then, summing the two input signals leads to responses that are approximately zero in the initial period; hence, the system may only be distinguishable for large values of $\bar{N}$.

The result in Proposition 1 validates the use of a frequency-based analysis in terms of absolute distinguishability. Hence, if the frequency contents of the input signal are know *a priori*, it is possible to infer whether or not a given fault will be detected.

3.4. Multiple-model adaptive control/set-valued observers architecture

Figure 5 depicts the fundamental MMAC architecture adopted in this article, referred to as MMAC/SVO architecture for time-varying systems, where N_S possible dynamic models for the system were considered. The main idea in this architecture is to have an SVO, referred to as *global SVO*, that is able to provide set-valued state estimates for all the admissible time-varying uncertainties of the plant, either nominal or faulty. Therefore, unless none of the N_S families of models – which assume that the uncertain parameters are time-varying – is able to describe the dynamics of the actual plant, the global SVO does never provide an empty set-valued estimate of the state. As

DOI: 10.1002/acs

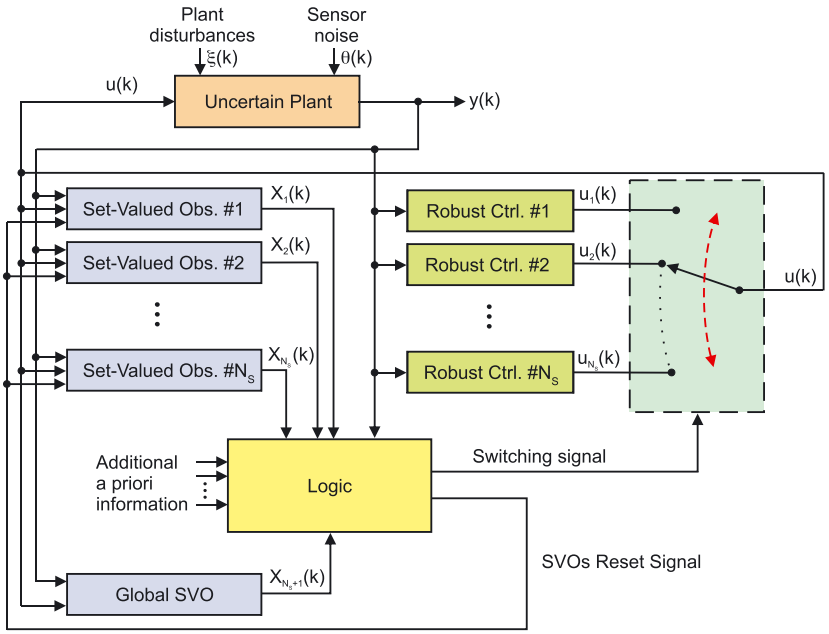

Figure 5. Multiple-model adaptive control/set-valued observers architecture for time-varying systems. X_i is the set-valued state estimate provided by set-valued observers #i.

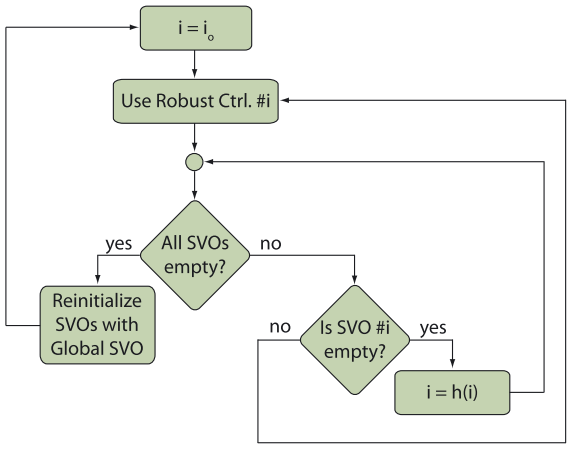

Figure 6. Algorithm for the *logic* block of the multiple-model adaptive control/set-valued observers architecture for time-invariant systems.

described in the sequel, this estimate is used to reinitialize the remaining SVOs when all the models are invalidated. Such an event occurs, for instance, when the impaired system recovers from a fault and, thus, retrieves its nominal behavior.

Indeed, as stressed in [30], in the case of time-varying plants, a model shall never be *disqualified* 'forever'. In fact, if the dynamics of the plant drift at a given time instant, then a previously discarded controller may be the appropriate one to be used from that moment on. Hence, the ability to address faulty-to-healthy transitions of the plant is an important feature of an FTC scheme.

The block entitled *Logic* in Figure 5 is responsible for selecting the controller to be connected to the loop, by taking into account the set-valued estimates of the state of the system provided by the SVOs. Several approaches can be used to tackle this decision problem. The one adopted in this article is depicted in Figure 6, where $h : \{2, \cdots, N_S\} \to \{1, 2, \cdots, N_S - 1\}$ is a map satisfying $h(n) = n - 1$, and $i_o = N_S$ is the number of controllers. This strategy takes into account the fact

DOI: 10.1002/acs

that, if $\rho \in \Omega_i$, then SVO #i does never fail, that is, the set-valued state estimate of the ith SVO, $\hat{X}_i(k)$, is never empty. On the other hand, if $\rho \notin \Omega_i$, then it can happen that, for some t_o, we have $\hat{X}_i(k) = \emptyset$, for all $k \geqslant t_o$.

In summary, the main strategy in the algorithm is to start by using any controller in the initial set of plausible controllers and then remove from the loop controllers whose corresponding models of the plant have been disqualified. For the sake of simplicity, the controllers are selected in a sequential fashion in this case, that is, if model $\#N_S$ is invalidated, we switch to controller $\#N_S - 1$, while if model $\#N_S - 1$ is invalidated, we switch to controller $\#N_S - 2$, and so on. However, other algorithms can be used, as long as the selected controller does never correspond to a previously *falsified* (or invalidated) model. In terms of FTC, it may be useful to initialize the algorithm with the controller designed for the healthy plant. This, however, is not a requirement of the algorithm, as discussed in the sequel.

If all but the global SVO provide empty set-valued state estimates for the plant, it means that none of the N_S models is able to describe the observed input/output data in the whole time-range. Thus, we conclude that the dynamics of the plant have drifted from one region of uncertainty to another, and hence, all the other SVOs should be reinitialized.

In order to ensure closed-loop stability, we posit the following assumptions.

Assumption 1
Let $\mathcal{S}$ be the (finite) set of *admissible* models of the plant. If $S_i \in \mathcal{S}$ and $S_j \in \mathcal{S}$, with $S_i \neq S_j$, then S_i and S_j are absolutely (X_o, U, W)-input distinguishable in N sampling times.

Assumption 2
Let:

(1) the initial state of the plant satisfy $x(0) \in X_o$;
(2) the control input sequence satisfy $u(j) \in U$ for all $j \geqslant 0$; and
(3) the sequence of disturbances satisfy $(d(j), n(j)) \in W$ for all $j \geqslant 0$.

Assumption 3
There exists $T_{\min} > 0$ such that, if $\rho(k) \in \Omega_j$, then there exist time indexes k_1 and k_2 such that

(1) $|k_2 - k_1| \geqslant T_{\min}$;
(3) $k_1 \leqslant k \leqslant k_2$; and
(4) $\rho(\kappa) \in \Omega_j$ for all $\kappa \in [k_1,\ k_2]$.

In other words, Assumption 1 is used to guarantee that the models in $\mathcal{S}$ can be distinguished from each other (in the sense of Definition 1), while Assumption 2 ensures that the input signals sufficiently excite the system to enable distinguishability. The latter assumption is key for performance, even though it can be dropped if only closed-loop stability is required, as described in [30]. Finally, Assumption 3 guarantees that the dynamics of the system to be controlled is *sufficiently slow*, so that the identification subsystem in Figure 5 is able to select the appropriate model of the plant. It is also related to the concept of *dwell-time*, which is key in many MMAC strategies, in order to ensure closed-loop stability – see, for instance, [21].

From these assumptions, we can conclude the following result.

Theorem 1 ([39]*)*
Consider a dynamic system, S_r, described by (4), such that $\rho(k) \in \Omega = \Omega_1 \cup \cdots \cup \Omega_{N_S}$. Suppose Assumptions 1–3 are satisfied and that controller, K_i, designed for the region of uncertainty Ω_i, asymptotically stabilizes the system (4) with $\rho \in \Omega_i$. Then, the closed-loop system with the MMAC/SVO architecture for time-varying plants is input/output stable, for sufficiently large $T_{\min}$.

This result provides guarantees that the closed-loop system is stable, for *sufficiently slow* time-variations of the dynamics. The proof of the theorem (that is fully described in [39, 54]) can be sketched as follows:

(1) Given Assumptions 1 and 2, we can guarantee that, if the dynamics of the plant remain modeled by the same LPV description for a sufficiently large time interval, the SVOs will be able to invalidate all but the 'correct' model of the plant.

DOI: 10.1002/acs

(2) Assumption 3 ensures that indeed the dynamics of the system remains in the same region of uncertainty for a sufficiently large time interval.
(3) Because each *local* controller is guaranteed to asymptotically stabilize the system for the corresponding region of uncertainty, and using similar arguments to those in [30], it can be shown that the closed-loop system is stable.

Remark 5
As shown in [30], the minimum value of $T_{\min}$ required to ensure stability increases with the number of admissible models, N_S. Therefore, the appropriate selection of this set of models is of prime importance in order to guarantee that the transients caused by the model identification process are small, and thus that the closed-loop performance is not severely degraded. As described in the sequel, the distinguishability concept is adopted for this purpose, because it allows the definition of this set of models, based on the maximum time allowed for model identification, and on the intensity of the exogenous signals that excite the plant.

3.5. Multiple-model adaptive control/set-valued observer applied to fault-tolerant control of an air heating fan

The dynamics in (4) can be readily transformed into the model described by (6), where the offset, $b_i(\cdot)$, is modeled by a low-frequency disturbance, added to the measured output of the system. In particular, $b_i(\cdot)$ is described by

$$b_i(k+1) = 0.999 b_i(k) + 0.0010 u_b(k),$$

where $u_b(k)$ is drawn from an interval with pre-specified bounds. The SVOs allow the definition of (time-varying) upper and lower bounds for this disturbance that can aid the invalidation of the models. However, because of the large level of uncertainty of this offset, which is highly dependent on the room temperature, we assume that the aforementioned upper and lower bounds correspond to the upper and lower saturation levels of the temperature sensor, respectively.

In designing the SVO-based FTC system for the air heating fan, $N_S = 4$ models are considered, where the last one, S_4, is used by the *global* SVO, as described in the previous subsection. The remaining models are obtained for the throttle openings in Table I. Each model is described by (6), with

$$A_1(\rho) = \begin{bmatrix} 1.3467 & 1 & 0 & 0 \\ -0.6635 & 0 & 1 & 0 \\ 0.1504 & 0 & 0 & 0 \\ 0 & 0 & 0 & 0.9990 \end{bmatrix} + \rho_1 \begin{bmatrix} -0.1132 & 0 & 0 & 0 \\ 0.1235 & 0 & 0 & 0 \\ -0.0349 & 0 & 0 & 0 \\ 0 & 0 & 0 & 0 \end{bmatrix}, \; B_1(\rho) = \begin{bmatrix} 0.0147 \\ 0.1166 \\ 0 \\ 0 \end{bmatrix} + \rho_2 \begin{bmatrix} 0.0046 \\ 0.0096 \\ 0 \\ 0 \end{bmatrix},$$

$$A_2(\rho) = \begin{bmatrix} 0.7911 & 1 & 0 & 0 \\ -0.1268 & 0 & 1 & 0 \\ 0.0160 & 0 & 0 & 0 \\ 0 & 0 & 0 & 0.9990 \end{bmatrix} + \rho_1 \begin{bmatrix} -0.0814 & 0 & 0 & 0 \\ 0.0589 & 0 & 0 & 0 \\ -0.0109 & 0 & 0 & 0 \\ 0 & 0 & 0 & 0 \end{bmatrix}, \; B_2(\rho) = \begin{bmatrix} 0.0677 \\ 0.0830 \\ 0 \\ 0 \end{bmatrix} + \rho_2 \begin{bmatrix} 0.0092 \\ -0.0269 \\ 0 \\ 0 \end{bmatrix},$$

$$A_3(\rho) = \begin{bmatrix} 0.7878 & 1 & 0 & 0 \\ -0.1806 & 0 & 1 & 0 \\ 0.0534 & 0 & 0 & 0 \\ 0 & 0 & 0 & 0.9990 \end{bmatrix} + \rho_1 \begin{bmatrix} 0.0129 & 0 & 0 & 0 \\ -0.0399 & 0 & 0 & 0 \\ 0.0236 & 0 & 0 & 0 \\ 0 & 0 & 0 & 0 \end{bmatrix}, \; B_3(\rho) = \begin{bmatrix} 0.0768 \\ 0.0488 \\ 0 \\ 0 \end{bmatrix} + \rho_2 \begin{bmatrix} 0.0013 \\ -0.0040 \\ 0 \\ 0 \end{bmatrix},$$

$$A_4(\rho) = \begin{bmatrix} 1.0117 & 1 & 0 & 0 \\ -0.3588 & 0 & 1 & 0 \\ 0.0799 & 0 & 0 & 0 \\ 0 & 0 & 0 & 0.9990 \end{bmatrix} + \rho_1 \begin{bmatrix} -0.9888 & 0 & 0 & 0 \\ 1.0404 & 0 & 0 & 0 \\ -0.2853 & 0 & 0 & 0 \\ 0 & 0 & 0 & 0 \end{bmatrix}, \; B_4(\rho) = \begin{bmatrix} 0.0488 \\ -0.0887 \\ 0 \\ 0 \end{bmatrix} + \rho_2 \begin{bmatrix} 0.0653 \\ -0.0430 \\ 0 \\ 0 \end{bmatrix},$$

and

$$C_1 = C_2 = C_3 = C_4 = \begin{bmatrix} 1 & 0 & 0 & 1 \end{bmatrix},$$

DOI: 10.1002/acs

Table I. Admissible throttle openings for each model.

Model	Throttle opening (θ)	Plant condition
S_1	[10°, 60°[	Faulty
S_2	[60°, 120°]	Healthy
S_3	]120°, 135°]	Faulty

$$L_1 = L_2 = L_3 = L_4 = \begin{bmatrix} 0 \\ 0 \\ 0 \\ 0.0010 \end{bmatrix}, \quad N_1 = N_2 = N_3 = N_4 = 0.1,$$

where the uncertain vector of parameter, $\rho = (\rho_1, \rho_2)$, is related to the unknown throttle opening, as described in the sequel, and where the exogenous disturbances and measurement noise satisfy, respectively,

$$0 \leqslant d(k) \leqslant 9, \quad |n(k)| \leqslant 1.$$

These models are obtained by constructing a grid of systems, each of which with the *ARMAX* structure defined in (1), and for a particular value of the throttle opening. As an example, for the class of models S_1, a set of N_1 models is generated by considering a set of N_1 equally spaced throttle openings. For each of these models, a state-space description as in (2) is derived and a pair $\left(\tilde{A}_1^j, \tilde{B}_1^j\right)$ is obtained, with $j \in \{1, \ldots, N_1\}$. Finally, an affine LPV representation for all $\left(\tilde{A}_1^j, \tilde{B}_1^j\right)$, $j \in \{1, \ldots, N_1\}$, is obtained by minimizing the element-wise mean squared error of

$$\begin{bmatrix} \tilde{A}_1^j \\ \\ \tilde{B}_1^j \end{bmatrix} - \left(\begin{bmatrix} \bar{A}_1^0 \\ \\ \bar{B}_1^0 \end{bmatrix} + \sum_{\ell=1}^{n_\rho} \begin{bmatrix} \bar{A}_1^\ell(\rho_\ell^j) \\ \\ \bar{B}_1^\ell(\rho_\ell^j) \end{bmatrix} \right),$$

where n_ρ is the number of independent parameters considered, and ρ_ℓ^j is the instantiation of parameter ℓ for the pair $\left(\tilde{A}_1^j, \tilde{B}_1^j\right)$. These parameters can be functions of *external variables*, such as the throttle opening. In the example considered, $\rho_1 = \theta$ and $\rho_2 = \theta^2$. The process is repeated for the remaining families of models, including that of the Global SVO, with the exception that, in the latter case, any admissible throttle opening in the interval [10°, 135°] is considered. Alternative methods may be used to generate this set of LPV models, as described, for instance, in [60–63] and references therein. A systematic procedure to address this problem is also provided in [64], based on linear fractional transformations (LFTs).

Remark 6
The uncertainty in each model is essentially a consequence of the unknown throttle opening. However, two independent uncertain parameters, ρ_1 and ρ_2, are considered by the SVOs, because the methodology adopted to their implementation [39] disregards any relationship between the uncertain parameters of $A(\rho)$ and $B(\rho)$. As a result, the set-valued state estimates provided by the SVOs are conservative, in the sense that they may include states that are not compatible with the dynamics of the plant.

Each model obtained for a throttle opening between 60° and 120° is considered a non-faulty setup. Hence, if the dynamics of the system are well-described by S_2, then the system is considered to be operating normally. If, however, the observed sequence of input/output signals is not compatible with S_2, but rather with S_1 or S_3, then the system is faulty and a controller for the impaired systems should be connected to the loop.

In order to evaluate the conditions in which a given fault is detected, the distinguishability of the faulty and nominal models can be evaluated. As an example, Figure 7 depicts the minimum amplitude of the control signal as a function of the frequency, that guarantees absolute input distinguishability of S_1, for different values of the SVOs horizon, N. Therefore, if, for example, the input

DOI: 10.1002/acs

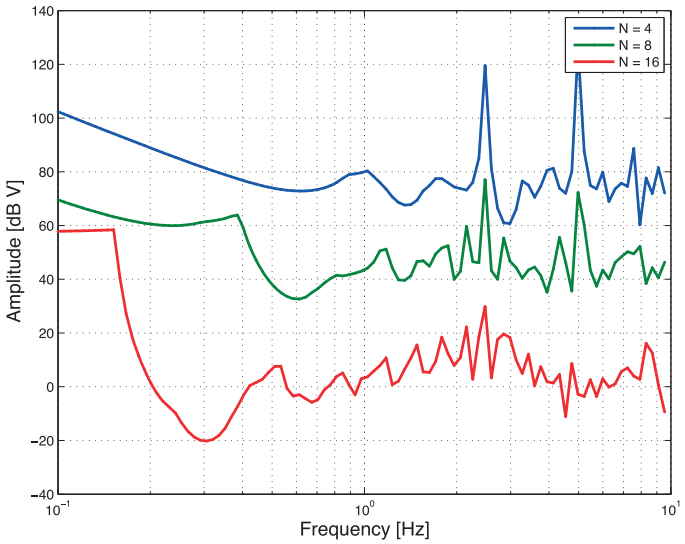

Figure 7. Minimum amplitude of the control signal as a function of the frequency, that guarantees absolute input distinguishability of S_1, for different values of the set-valued observers horizon, N.

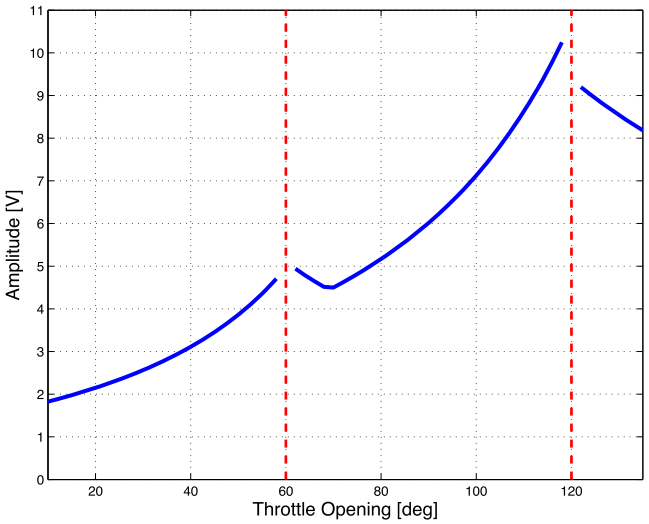

Figure 8. Minimum amplitude of the control signal as a function of the actual value of the throttle opening, that guarantees absolute input distinguishability of the three models, for $N = 20$. The control signal is assumed to be sinusoidal, with frequency 0.1 Hz.

signal is a sinusoid with amplitude 0.1 V and frequency 0.3 Hz, the fault is detected in, at most, 16 sampling periods, that is, in 3.2 s. This result is obtained by using the approach described in [5].

A complementary analysis can be performed by fixing the control input signal, and varying the actual throttle opening, as illustrated in Figure 8. As expected, for values of the throttle opening closer to the boundaries of each region, it is, in general, harder to identify the model of the system.

These results can be interpreted as follows. If the performance of the closed-loop is deteriorated (or if, ultimately, the system becomes unstable), the magnitude of the control signal tends to increase. The results in Figure 8, however, indicate that input signals with larger amplitudes facilitate the distinguishability of the systems, that is, reduces the time required to detect – and compensate for – faults.

As described in [65], the local non-adaptive controllers for each region of the dynamics of the system were designed so as to minimize the $\mathcal{H}_2$-norm of the tracking error – see [66] – and are

DOI: 10.1002/acs

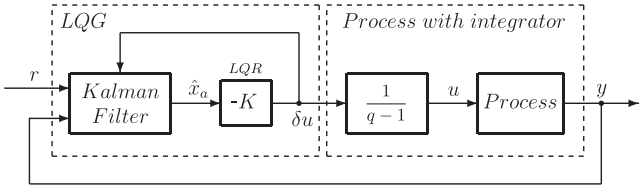

Figure 9. Interconnection between the plant and the linear quadratic Gaussian controller.

typically referred to as linear quadratic Gaussian (LQG) controllers. For further details on the design choices and specifications, the reader is referred to [65].

In order to avoid chattering due to switching of the controllers, an integrator is connected to the loop, in between the controller and the plant – see [67]. In terms of controller design, it can be assumed that the integrator is part of the process. Figure 9 depicts the LQG controller (that can be seen as the combination of a linear quadratic regulator (LQR), and a Kalman filter (KF), based on the separation principle [68]), together with the augmented process (plant and integrator).

The augmented process is, therefore, described by

$$\begin{aligned} \underbrace{\begin{bmatrix} x(k+1) \\ u(k+1) \end{bmatrix}}_{x_a(k+1)} &= \underbrace{\begin{bmatrix} A_i & B_i \\ 0 & 1 \end{bmatrix}}_{\bar{A}_i} \underbrace{\begin{bmatrix} x(k) \\ u(k) \end{bmatrix}}_{x_a(k)} + \underbrace{\begin{bmatrix} 0 \\ 1 \end{bmatrix}}_{\bar{B}_i} \delta u(k) \\ y(k) &= \underbrace{\begin{bmatrix} C_i & 0 \end{bmatrix}}_{\bar{C}_i} \begin{bmatrix} x(k) \\ u(k) \end{bmatrix} \end{aligned}, \tag{10}$$

where x_a is the augmented state, $\bar{A}_i$, $\bar{B}_i$, and $\bar{C}_i$ are the augmented matrices, and δu is the incremental command action from the controller. For the sake of simplicity, the disturbances are omitted in this description. The design of the LQG controllers is performed using the quadratic cost function

$$J(\delta u) = \lim_{N\to\infty} \sum_{k=0}^{N-1} \left(e^2(k) + R\,[\delta u(k)]^2 \right), \tag{11}$$

where $e(k) = r - y(k)$ is the tracking error and $R > 0$ is a weighting matrix. For $N \to \infty$, the discrete-time LQG controller for model #i is, finally, described by

$$\begin{cases} \hat{x}_a(k+1) = \left(\bar{A}_i - \bar{B}_i \mathfrak{K}_i - \mathfrak{L}_i \bar{C}_i\right) \hat{x}_a(k) - \mathfrak{L}_i e(k) \\ \delta u(k) \quad = -\mathfrak{K}_i \hat{x}_a(k) \end{cases}, \tag{12}$$

where $\mathfrak{L}_i$ and $\mathfrak{K}_i$ are the observer and regulator gains, respectively. An anti-windup block was also designed to avoid transients caused by saturation of the command input.

Remark 7

In designing these controllers, the offset b_i is regarded as a (low-frequency) disturbance that is naturally rejected by the inclusion of the integrator at the plant input, and the plant is considered time-invariant.

4. EXPERIMENTAL RESULTS

Using the Process Trainer PT326, depicted in Figure 10, a series of tests have been performed in order to experimentally evaluate the behavior of the proposed control methodology. We start by analyzing the behavior of the local controllers, synthesized as described in Section 3.5, followed by the setup description and performance evaluation of the proposed SVO-based FTC method.

DOI: 10.1002/acs

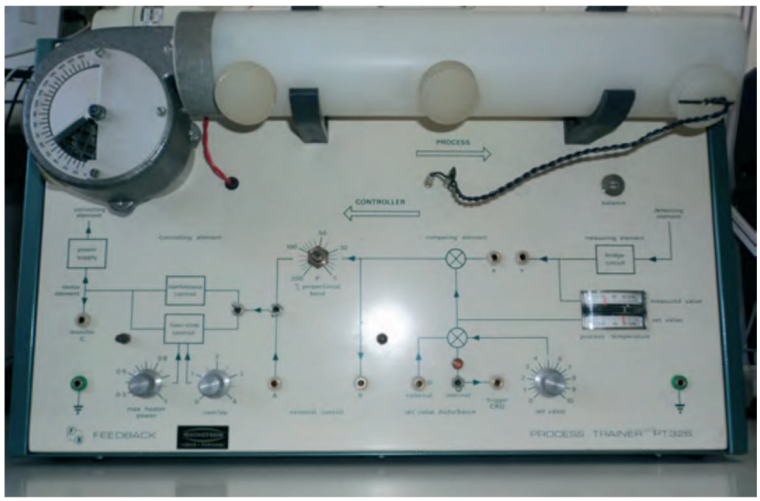

Figure 10. Process Trainer PT326 experimental setup.

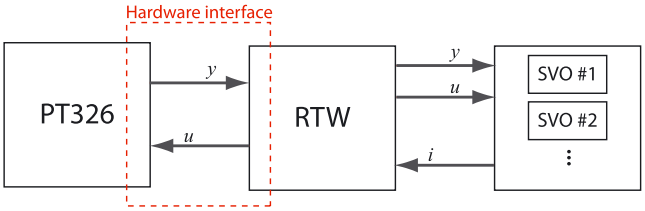

Figure 11. Experimental setup: (1) PT326 air heating fan, (2) computer with the Real-Time Workshop toolbox, and (3) computer implementing the set-valued observers routines and indicating the selected model, i.

Throughout this section, we consider three local models for the plant, resulting from the throttle openings $\theta_1 = 30°$, $\theta_2 = 70°$, and $\theta_3 = 130°$. We denote by $\tilde{S}_i$ the model of the system for $\theta = \theta_i$, and by K_i the associated LQG controller. Therefore, $\tilde{S}_2$ represents a non-faulty model of the plant, while the other two describe faulty situations.

4.1. Description of the experimental setup

The experimental setup used to evaluate the adopted SVO-based FTC methodology and illustrated in Figure 11, is composed of

(1) the Process Trainer PT326 experimental device (Figure 10);
(2) a computer equipped with MATLAB's Real-Time Workshop (RTW) toolbox; and
(3) a computer implementing the SVOs routines.

The computer with the RTW toolbox implements the interface between the air heating fan and the control algorithm. It is responsible for acquiring the sensor data and generating the control input signals. The computer that implements the SVOs routines collects all this information and generates set-valued state estimates for each plausible model of the system. Notice that, as illustrated in Figure 5, these are highly parallelizable algorithms, thus being able to take advantage of parallel processing architectures – such as multi-core processing units – and being implemented in a distributed fashion. These two computers communicate between themselves by interchanging user datagram protocol (UDP) packets.

4.2. Experimental evaluation of the local controllers

The reference tracking performance of each controller can be evaluated by resorting to Figure 12. In these experiments, we assume that the appropriate local controller is connected to the loop. Notice

DOI: 10.1002/acs

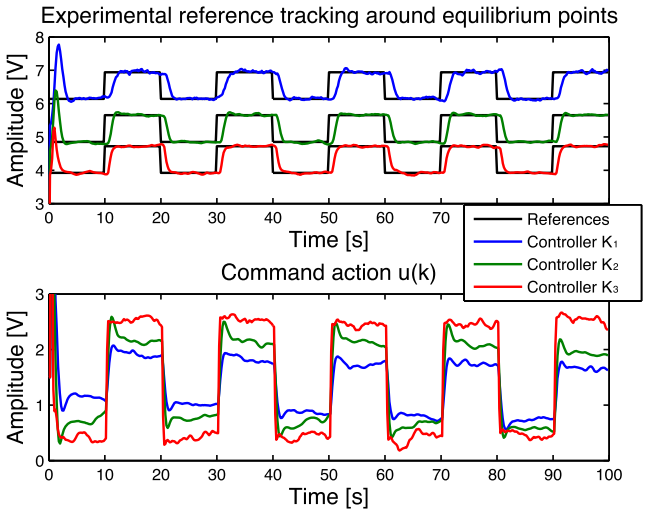

Figure 12. Experimental closed-loop results for the different equilibrium points ($\theta_1 = 30°$, $\theta_2 = 70°$, and $\theta_3 = 130°$), using for each one the corresponding local controller.

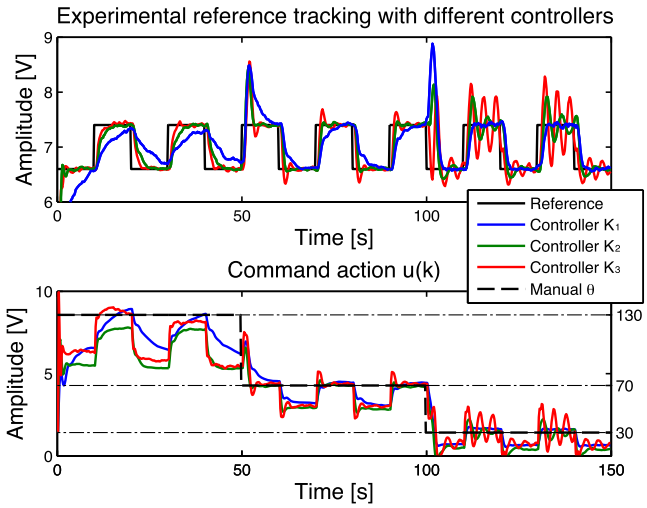

Figure 13. Experimental closed-loop results for a time-varying throttle opening, using the three local controllers, each one in a different experiment.

that, due to the aforementioned overheating of the tube, the control action decreases as time goes by. This effect is particularly notorious for controllers K_2 and K_3. Indeed, as the temperature of the tube increases, the control input effort required to achieve the same air temperature is reduced.

In the following experiments, we consider that the throttle opening is changed manually every 50 secs, according to the sequence 130°, 70° and 30°. Moreover, only a single LQG controller is used in each experiment. The results are summarized in Figure 13.

It should be noticed that none of the controllers exhibits reasonable performance for the whole range of the throttle opening, which indicates that non-adaptive control strategies may not be suitable for the problem at hand. This means that if the possibility of having system failures is not considered in the design of the controllers, the closed-loop performance may be severely affected.

4.3. Experimental evaluation of the SVO-based FTC system

Figure 14 illustrates a typical time-sequence of the results obtained using the SVO-based FTC method described in this paper. The throttle opening changes every 70 secs. In this case, the SVOs

DOI: 10.1002/acs

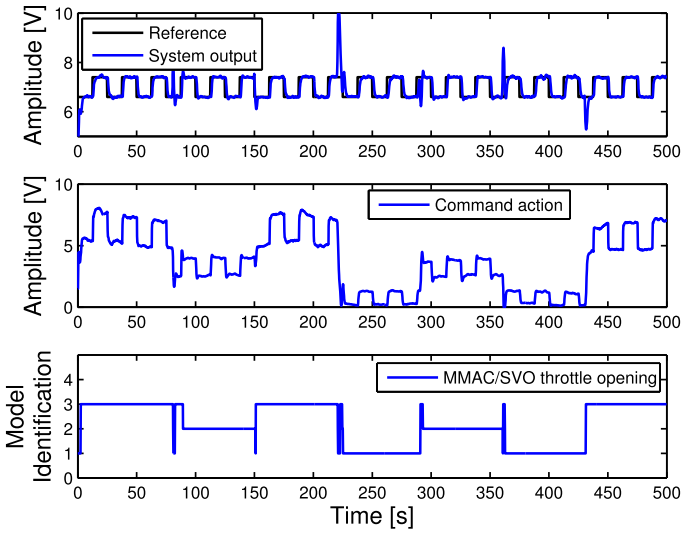

Figure 14. Experimental results for the closed-loop system with the multiple-model adaptive control/set-valued observers.

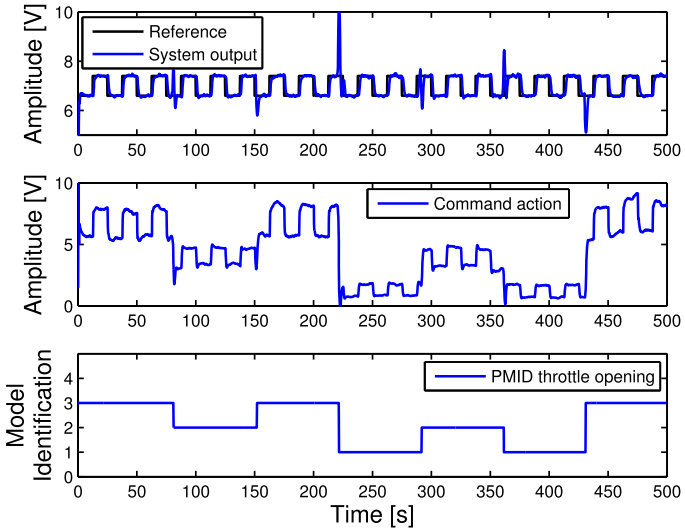

Figure 15. Experimental results for the closed-loop system with the perfect model identification (unrealizable in practical situations).

take typically less than 10 secs to invalidate all but the 'correct' model of the system. This is valid both for fault detection and for recovery from faults. As a consequence, the tracking error is small, except during the transients between the switching of the non-adaptive controllers.

The results were also compared, through a series of experiments, with the so-called *Perfect Model IDentification* method. In this scheme, the appropriate controller is connected to the loop, by taking advantage of the information regarding the throttle opening. This method, of course, cannot be implemented in practice, because such information is assumed not to be available for the controller and hence is used here just for evaluating the results obtained.

As depicted in Figure 15, the results obtained with the Perfect Model IDentification method are similar to those of the SVO-based FTC system. In fact, the tracking error and the control input are comparable, although the MMAC/SVO shows slightly larger transients during the changes of the throttle opening. In terms of root mean square (RMS) tracking error, the results obtained with both approaches are summarized in Table II, for seven repetitions of the same experimental test.

DOI: 10.1002/acs

Table II. RMS of the output.

	RMS (°C)
PMID	1.05
MMAC/SVO	1.07

PMID, Perfect Model IDentification; MMAC/SVO, multiple-model adaptive control/set-valued observer.

It should be noticed that the deterioration, in terms of RMS performance, that comes from the use of the SVO-based decision subsystem, is nearly 2%, for the scenario considered. Therefore, these results indicate that the technique proposed is potentially applicable in practical FTC problems, with clear benefits in terms of improved performance.

5. CONCLUSIONS

This paper described the application of the MMAC methodology using SVOs to the problem of FTC of an air heating fan. The concept of absolute distinguishability was adopted to evaluate the input signals that promote the detection of faults.

The behavior of the proposed methodology was experimentally evaluated and it was shown that, at least for the scenarios considered, the deterioration in terms of RMS performance due to the SVO-based model selection is around 2%. As a shortcoming, the computational requirements of the SVOs are typically large when compared with the ones of a passive FTC system. Nevertheless, for the present case, this did not jeopardize the practical implementability of the technique, as the sampling period of 200 ms was sufficient to perform all the calculations.

APPENDIX

Lemma 1
Let $\omega_1, \omega_2 \in \mathbb{R}^+$, with $\omega_2 > \omega_1$, and $\phi_1, \phi_2 \in \mathbb{R}$. Then,

$$\lim_{T\to\infty} \frac{1}{T} \int_0^\infty (\sin(\omega_1 t + \phi_1) - \sin(\omega_2 t + \phi_2))^2 \, dt = 1$$

Proof

$$\begin{aligned}
&\textstyle\int_0^\infty (\sin(\omega_1 t + \phi_1) - \sin(\omega_2 t + \phi_2))^2 \, dt = \\
&\quad = \textstyle\int_0^\infty (\sin(\omega_1 t + \phi_1))^2 \, dt + \int_0^\infty (\sin(\omega_2 t + \phi_2))^2 \, dt - 2\int_0^\infty \sin(\omega_1 t + \phi_1)\sin(\omega_2 t + \phi_2) dt \\
&\quad = \tfrac{T}{2} + \tfrac{\sin(2\phi_1) - \sin(2\omega_1 T + 2\phi_1)}{4\omega_1} + \tfrac{T}{2} + \tfrac{\sin(2\phi_2) - \sin(2\omega_2 T + 2\phi_2)}{4\omega_2} + \\
&\qquad + \tfrac{-\sin(\phi_1 - \phi_2) + \sin(\phi_1 - \phi_2 + (\omega_1 - \omega_2)T)}{\omega_1 - \omega_2} + \tfrac{\sin(\phi_1 + \phi_2) - \sin(\phi_1 + \phi_2 + (\omega_1 + \omega_2)T)}{\omega_1 + \omega_2}.
\end{aligned}$$

Hence,

$$\lim_{T\to\infty} \tfrac{1}{T} \textstyle\int_0^\infty (\sin(\omega_1 t + \phi_1) - \sin(\omega_2 t + \phi_2))^2 \, dt = \tfrac{1}{2} + \tfrac{1}{2} = 1.$$

□

ACKNOWLEDGEMENTS

Part of this work has been supported by FCT under project ARGUS – Activity Recognition and Object Tracking Based on Multiple Models, contract PTDC/EEA-CRO/098550/2008, national funds through UID/CEC/50021/2013, LARSYS funding through FCT [UID/EEA/50009/2013], and project MYRG117(Y1-L3)-FST12-MKM of the University of Macau.

DOI: 10.1002/acs

REFERENCES

1. Ducard G. *Fault-Tolerant Flight Control and Guidance Systems: Practical Methods for Small Unmanned Aerial Vehicles*, Advances in Industrial Control. Springer: London, UK, 2009.
2. Hwang I, Kim S, Kim Y, Eng Seah C. A survey of fault detection, isolation and reconfiguration methods. *IEEE Transactions on Control Systems Technology* 2010; **18**(3):636–653.
3. Blanke M, Kinnaert M, Lunze J, Staroswiecki M, Schröder J. *Diagnosis and Fault-tolerant Control* (2nd edn). Springer: Berlin, Germany, 2006.
4. Jiang J, Yu X. Fault-tolerant control systems: a comparative study between active and passive approaches. *Annual Reviews in Control* 2012; **36**(1):60–72.
5. Rosa P, Casau P, Silvestre C, Tabatabaeipour SM, Stoustrup J. A set-valued approach to FDI and FTC: theory and implementation issues. *8th IFAC Symposium on Fault Detection, Supervision and Safety of Technical Processes*, Mexico City, Mexico, 2012; 1281–1286.
6. Anderson B, Brinsmead T, Liberzon D, Stephen Morse A. Multiple model adaptive control with safe switching. *International Journal of Adaptive Control and Signal Processing* 2001; **15**(5):445–470.
7. Patton RJ. Fault-tolerant control systems: the 1997 situation. *IFAC Symposium on Fault Detection Supervision and Safety for Technical Processes*, Vol. 3, Kingston Upon Hull, UK, 1997; 1033–1054.
8. Feedback Instruments Ltd., *Process Trainer PT 326*.
9. Rosa P, Silvestre C, Shamma JS, Athans M. Multiple-model adaptive control with set-valued observers. *Proceedings of the 48th IEEE Conference on Decision and Control*, Shanghai, China, December 2009; 2441–2447.
10. Rosa P, Silvestre C, Athans M. Model falsification of LPV systems using set-valued observers. *Proceedings of the 18th IFAC World Congress*, Milano, Italy, August–September 2011; 1546–1551.
11. Rosa P, Silvestre C. Fault detection and isolation of LPV systems using set-valued observers: an application to a fixed-wing aircraft. *Control Engineering Practice* 2013; **21**(3):242–252.
12. Rosa P, Simao T, Lemos JM, Silvestre C. Multiple-model adaptive control of an air heating fan using set-valued observers. In *2012 20th Mediterranean Conference on Control & Automation (MED)*. IEEE: Barcelona, Spain, 2012; 469–474.
13. Narendra K, Annaswamy A. *Stable Adaptive Systems*. Prentice Hall, Inc.: NJ, USA, 1988.
14. Åström K, Wittenmark B. *Adaptive Control* (2nd edn). Addison-Wesley: MA, USA, 1995.
15. Landau I. *Adaptive Control: The Model Reference Approach*. Marcel Dekker: NY, USA, 1979.
16. Sastry S, Sun J. *Adaptive Control: Stability, Convergence and Robustness*. Prentice-Hall: NJ, USA, Englewood Cliffs, 1989.
17. Ioannou P, Sun J. *Robust Adaptive Control*. Prentice Hall, Inc.: Upper Saddle River, New Jersey, USA, 1996.
18. Maybeck P. *Stochastic Models, Estimation and Control*. Academic Press: USA, 1979 and 1982, vol. I and II.
19. Kuipers M, Ioannou P. Multiple model adaptive control with mixing. *IEEE Transactions on Automatic Control* 2010; **55**(8):1822–1836.
20. Fekri S, Athans M, Pascoal A. Robust multiple model adaptive control (RMMAC): a case study. *International Journal of Adaptive Control and Signal Processing* 2006; **21**(1):1–30.
21. Hespanha JP, Liberzon D, Morse AS, Anderson B, Brinsmead T, de Bruyne F. Multiple model adaptive control, part 2: switching. *International Journal of Robust and Nonlinear Control,* Special Issue on Hybrid Systems in Control 2001; **11**(5):479–496.
22. Ahmed-Zaid F, Ioannou P, Gousman K, Rooney R. Accommodation of failures in the flight control system of the F-16 aircraft using adaptive control. In *American Control Conference*. IEEE: San Diego, California, USA, 1990; 764–769.
23. Napolitano MR, Neppach C, Casdorph V, Naylor S, Innocenti M, Silvestri G. Neural-network-based scheme for sensor failure detection, identification, and accommodation. *Journal of Guidance, Control, and Dynamics* 1995; **18**(6):1280–1286.
24. Bodson M, Groszkiewicz JE. Multivariable adaptive algorithms for reconfigurable flight control. *IEEE Transactions on Control Systems Technology* 1997; **5**(2):217–229.
25. Aström K, Albertos P, Blanke M, Isidori A, Schaufelberger W, Sanz R. *Control of Complex Systems*. Springer: London, UK, 2012.
26. Fekri S, Athans M, Pascoal A. Issues, progress and new results in robust adaptive control. *International Journal of Adaptive Control and Signal Processing* 2006; **20**:519–579.
27. Rosa P, Shamma JS, Silvestre C, Athans M. Stability overlay for linear and nonlinear time-varying plants. *Proceedings of the 48th IEEE Conference on Decision and Control*, Shanghai, China, December 2009; 2435–2440.
28. Hassani V, Hespanha JP, Athans M, Pascoal A. Stability analysis of robust multiple model adaptive control. *Proceedings of the 18th IFAC World Congress*, Milano, Italy, August–September 2011; 350–355.
29. Al-Shyoukh I, Shamma JS. Switching supervisory control using calibrated forecasts. *IEEE Transactions on Automatic Control* 2009; **54**(4):705–716.
30. Rosa P, Shamma JS, Silvestre C, Athans M. Stability overlay for adaptive control laws. *Automatica* May 2011; **47**(5):1007–1014.
31. Baldi S, Battistelli G, Mosca E, Tesi P. Multi-model unfalsified adaptive switching supervisory control. *Automatica* 2010; **46**(2):249–259.
32. Manuelli G, Mosca E, Safonov M, Tesi P. Unfalsified virtual reference adaptive switching control of plants with persistent disturbances. *Proceedings of the IFAC World Congress*, Seoul, Korea, July 2008; 8925–8930.

DOI: 10.1002/acs

33. Safonov M, Tsao T-C. The unfalsified control concept: a direct path from experiment to controller. In *Feedback Control, Nonlinear Systems and Complexity*, Francis BA, Tannenbaum AR (eds). Springer-Verlag: Berlin, 1995; 196–214.
34. Safonov M, Tsao T-C. The unfalsified control concept and learning. *IEEE Transactions on Automatic Control* 1997; **42**(6):843–847.
35. Wang R, Paul A, Stefanovic M, Safonov M. Cost-detectability and stability of adaptive control systems. *International Journal of Robust and Nonlinear Control* 2007; **17**(5–6):549–561.
36. Angeli D, Mosca E. Lyapunov-based switching supervisory control of nonlinear uncertain systems. *IEEE Transactions on Automatic Control* 2002; **47**:500–505.
37. Wang D, Paul A, Stefanovic M, Safonov M. Cost-detectability and stability of adaptive control systems. *Proceeding of the 44th IEEE International Conference on Decision and Control*, Seville, Spain, December 2005; 3584–3589.
38. Lourenço JM, Lemos JM. Predictive adaptive control of plants with online structural changes based on multiple models. *International Journal of Adaptive Control and Signal Processing* 2008; **22**:774–794.
39. Rosa P, Silvestre C. Multiple-model adaptive control using set-valued observers. *International Journal of Robust and Nonlinear Control* 2013; **24**:2490–2511.
40. Rosa P, Silvestre C, Athans M. Model falsification using set-valued observers for a class of discrete-time dynamic systems: a coprime factorization approach. *International Journal of Robust and Nonlinear Control* 2013; **24**: 2928–2942.
41. Schweppe F. Recursive state estimation: unknown but bounded errors and system inputs. *IEEE Transactions on Automatic Control* 1968; **13**(1):22–28.
42. Schweppe F. *Uncertain Dynamic Systems*. Prentice-Hall: USA, 1973.
43. Yang F, Yongmin L. Set-membership filtering for discrete-time systems with nonlinear equality constraints. *IEEE Transactions on Automatic Control* 2009; **54**(10):2480–2486.
44. Baglietto M, Battistelli G, Scardovi L. Active mode observation of switching systems based on set-valued estimation of the continuous state. *International Journal of Robust and Nonlinear Control* 2009; **19**:1521–1540.
45. Lin H, Zhai G, Antsaklis PJ. Set-valued observer design for a class of uncertain linear systems with persistent disturbance and measurement noise. *International Journal of Control* 2003; **76**(16):1644–1653.
46. Jaulin L. Robust set-membership state estimation; application to underwater robotics. *Automatica* 2009; **45**(1): 202–206.
47. Raıssi T, Ramdani N, Candau Y. Set membership state and parameter estimation for systems described by nonlinear differential equations. *Automatica* 2004; **40**(10):1771–1777.
48. Puig V. Fault diagnosis and fault tolerant control using set-membership approaches: application to real case studies. *International Journal of Applied Mathematics and Computer Science* 2010; **20**(4):619–635.
49. Combastel C, Zhang Q. Robust fault diagnosis based on adaptive estimation and set-membership computations. *Fault Detection, Supervision and Safety of Technical Processes* 2006; **6**(1):1204–1209.
50. Efimov D, Perruquetti W, Raïssi T, Zolghadri A. Interval observers for time-varying discrete-time systems. *IEEE Transactions on Automatic Control* 2013; **58**(12):3218–3224.
51. Mazenc F, Kieffer M, Walter E. Interval observers for continuous-time linear systems with discrete-time outputs. In *American Control Conference (ACC)*. IEEE: Montreal, Canada, 2012; 1889–1894.
52. Shamma JS, Tu K-Y. Set-valued observers and optimal disturbance rejection. *IEEE Transactions on Automatic Control* 1999; **44**(2):253–264.
53. Keerthi S, Gilbert E. Computation of minimum-time feedback control laws for discrete-time systems with state-control constraints. *IEEE Transactions on Automatic Control* 1987; **32**(5):432–435.
54. Rosa P. Multiple-model adaptive control of uncertain LPV systems. *Ph.D. Dissertation*, Instituto Superior Técnico, Lisbon, Portugal, 2011.
55. Rosa P, Silvestre C, Shamma JS, Athans M. Fault detection and isolation of LTV systems using set-valued observers. *Proceedings of the 49th IEEE Conference on Decision and Control*, Atlanta, GA, USA, December 2010; 768–773.
56. Rosa P, Silvestre C. On the distinguishability of discrete linear time-invariant dynamic systems. *Proceedings of the 50th IEEE Conference on Decision and Control*, Orlando, FL, USA, December 2011; 3356–3361.
57. Grewal M, Glover K. Identifiability of linear and nonlinear dynamical systems. *IEEE Transactions on Automatic Control* 1976; **21**(6):833–837.
58. Walter E, Lecourtier Y, Happel J. On the structural output distinguishability of parametric models, and its relations with structural identifiability. *IEEE Transactions on Automatic Control* 1984; **29**(1):56–57.
59. Lou H, Si P. The distinguishability of linear control systems. *Nonlinear Analysis: Hybrid Systems* 2009; **3**:21–38.
60. Tóth R, Heuberger PS, Van den Hof PM. Asymptotically optimal orthonormal basis functions for LPV system identification. *Automatica* 2009; **45**(6):1359–1370.
61. van Wingerden J-W, Verhaegen M. Subspace identification of bilinear and LPV systems for open-and closed-loop data. *Automatica* 2009; **45**(2):372–381.
62. Casella F, Lovera M. LPV/LFT modelling and identification: overview, synergies and a case study. In *IEEE International Conference on Computer-Aided Control Systems, 2008. CACSD 2008*. IEEE: San Antonio, Texas, USA, 2008; 852–857.
63. Rugh W, Shamma JS. A survey of research on gain-scheduling. *Automatica* 2000; **36**:1401–1425.
64. Magni J-F. Linear fractional representation toolbox for use with MATLAB, 2006. (Available from: http://w3.onera.fr/smac/) [Accessed on 23 April 2015].

DOI: 10.1002/acs

65. Simão T. Multiple model identification in systems with variable dynamics. *Master's Thesis*, Instituto Superior Técnico, Technical University of Lisbon, Portugal, October 2011.
66. Zhou K, Doyle J, Glover K. *Robust Optimal Control*. Prentice Hall: Englewood Cliffs, New Jersey, USA, 1996.
67. Lemos JM, Rato LM, Mosca E. Integrating predictive and switching control: basic concepts and an experimental case study. *Nonlinear Model Predictive Control* 2000; **26,** Part I:181–190.
68. Franklin GF, Workman ML, Powell D. *Digital Control of Dynamic Systems*. Addison-Wesley Longman Publishing Co., Inc.: Menlo Park, California, USA, 1997.

DOI: 10.1002/acs